RESEARCH ARTICLE

Human Mutation

OFFICIAL JOURNAL
HGVS
HUMAN GENOME VARIATION SOCIETY
www.hgvs.org

Pathogenic Effects of Novel Mutations in the P-Type ATPase *ATP13A2* (*PARK9*) Causing Kufor-Rakeb Syndrome, a Form of Early-Onset Parkinsonism

Jin-Sung Park,[1] Prachi Mehta,[1] Antony A. Cooper,[2] David Veivers,[1] André Heimbach,[3] Barbara Stiller,[3] Christian Kubisch,[3,4] Victor S. Fung,[5] Dimitri Krainc,[6] Alan Mackay-Sim,[7] and Carolyn M. Sue[1]*

[1]*Department of Neurogenetics, Kolling Institute of Medical Research, Royal North Shore Hospital and the University of Sydney, St. Leonards, New South Wales, Australia;* [2]*Garvan Institute of Medical Research and the University of New South Wales, Darlinghurst, New South Wales, Australia;* [3]*Institute of Human Genetics, Center for Molecular Medicine Cologne, and Cologne Excellence Cluster on Cellular Stress Responses in Aging-Associated Diseases, University of Cologne, Cologne, Germany;* [4]*Institute of Human Genetics, University of Ulm, Ulm, Germany;* [5]*Department of Neurology, Westmead Hospital, Westmead, New South Wales, Australia;* [6]*Department of Neurology, Massachusetts General Hospital, Harvard Medical School, MassGeneral Institute for Neurodegeneration, Charlestown, Massachusetts;* [7]*National Adult Stem Cell Research Centre, Eskitis Institute for Cell and Molecular Therapies, School of Biomolecular and Physical Sciences, Griffith University, Queensland, Australia*

Communicated by Christine Van Broeckhoven

Received 8 February 2011; accepted revised manuscript 21 April 2011.
Published online 3 May 2011 in Wiley Online Library (www.wiley.com/humanmutation). DOI 10.1002/humu.21527

ABSTRACT: Kufor-Rakeb syndrome (KRS) is a rare form of autosomal recessive juvenile or early-onset, levodopa responsive parkinsonism and has been associated with mutations in *ATP13A2*(also known as *PARK9*), a lysosomal type 5 P-type ATPase. Recently, we identified novel compound heterozygous mutations, c.3176T>G (p.L1059R) and c.3253delC (p.L1085WfsX1088) in *ATP13A2* of two siblings affected with KRS. When overexpressed, wild-type ATP13A2 localized to Lysotracker-positive and LAMP2-positive lysosomes while both truncating and missense mutated ATP13A2 were retained in the endoplasmic reticulum (ER). Both mutant proteins were degraded by the proteasomal but not the lysosomal pathways. In addition, *ATP13A2* mRNA with c.3253delC was degraded by nonsense-mediated mRNA decay (NMD), which was protected by cycloheximide treatment. To validate our findings in a biologically relevant setting, we used patient-derived human olfactory neurosphere cultures and fibroblasts and demonstrated persistent ER stress by detecting upregulation of unfolded protein response-related genes in the patient-derived cells. We also confirmed NMD degraded *ATP13A2* c.3253delC mRNA in the cells. These findings indicate that these novel ATP13A2 mutations are indeed pathogenic and support the notion that mislocalization of the mutant ATP13A2, resultant ER stress, alterations in the proteasomal pathways and premature degradation of mutant *ATP13A2* mRNA contribute to the aetiology of KRS.
Hum Mutat 32:956–964, 2011. © 2011 Wiley-Liss, Inc.

KEY WORDS: Kufor-Rakeb syndrome; KRS; early-onset parkinsonism; ATP13A2; PARK9; proteasomal pathway; nonsense-mediated mRNA decay

Introduction

Parkinson disease (PD) is the most common movement disorder with affected patients showing signs of bradykinesia, tremor, rigidity, and postural instability. PD can be caused by both genetic and environmental factors. During the past decade, identification of genetic causes of familial PD has provided molecular insights into the pathophysiology underlying both familial and sporadic PD. More than 15 chromosomal loci have been identified and assigned as PARK1-15 [Hatano et al., 2009]. Mutations in several genes have been reported to cause monogenic forms of PD. Mutations in α-*synuclein* (*PARK1/4*) [Polymeropoulos et al., 1997] and *LRRK2* (*PARK8*) [Zimprich et al., 2004] follow an autosomal dominant pattern of inheritance while mutations in *Parkin* (*PARK2*) [Kitada et al., 1998], *DJ-1* (*PARK7*) [Bonifati et al., 2003], *PINK1* (*PARK6*) [Valente et al., 2004], and *ATP13A2* (*PARK9*) [Ramirez et al., 2006] follow an autosomal recessive pattern of inheritance.

ATP13A2 (MIM♯ 610513) has been assigned to Kufor-Rakeb Syndrome (KRS; MIM♯ 606693), a rare form of autosomal recessive juvenile or early-onset, levodopa-responsive type of parkinsonism. Other associated clinical manifestations of KRS include behavioral problems, facial tremor, pyramidal tract dysfunction, supranuclear gaze palsy, and dementia [Williams et al., 2005].

KRS has been associated with mutations in *ATP13A2*, a lysosomal type 5 P-type ATPase predicted to contain 10

Additional Supporting Information may be found in the online version of this article.

*Correspondence to: Carolyn M. Sue, Department of Neurology, Royal North Shore Hospital and Kolling Institute of Medical Research, University of Sydney, St. Leonards, NSW 2065. E-mail: c.sue@usyd.edu.au

Contract grant sponsors: The Australian Brain Foundation; The Parkinsons NSW Association (to C.M.S.); The Australian Department of Health and Aging (to C.M.S. and A.M.); The National Health and Medical Research Council of Australia; Contract grant number: 1010839 (to C.M.S. and A.A.C.); Contract grant sponsor: The Deutsche Forschungsgemeinschaft (to C.K.).

transmembrane domains (TM) [Schultheis et al., 2004]. To date, few families with KRS have been reported to have mutations in the *ATP13A2* [Behrens et al., 2010; Crosiers et al., 2011; Di Fonzo et al., 2007; Ning et al., 2008; Ramirez et al., 2006; Santoro et al., 2011; Schneider et al., 2010]. The function of ATP13A2 is still largely unknown, although putative pathogenic mechanisms that lead to neurodegeneration include loss of lysosomal function and abnormal protein aggregation.

We report a family of Asian descent with two siblings who had KRS and novel compound heterozygous mutations in *ATP13A2*. Functional studies showed that these were pathogenic mutations that resulted in the mutant protein being retained in the endoplasmic reticulum (ER) while the wild-type counterpart was located in the lysosome. Further studies indicated that the mutant protein was degraded by the proteasome, indicating that the proteasomal pathway is activated in this form of PD. In addition, mRNA with the mutation inducing a premature termination was degraded by nonsense-mediated mRNA decay (NMD).

Materials and Methods

Patients

A 22-year-old Asian male and his sister, born to nonconsanguinous parents, presented with juvenile-onset parkinsonism characterized by rigidity, tremor, and postural instability. The male proband had normal motor milestones but suffered mild developmental delay. He developed social anxiety by age 17, requiring treatment with selective serotonin reuptake inhibitors. He developed bilateral parkinsonism from age 19 with akinesia, rigidity, postural arm tremor without rest tremor, and postural instability. On examination he had a masked facies with a fine tremor of the lips and chin, worse on activation by pursing the lips. His speech was slurred. He had an inextinguishable glabellar tap. He had impaired upward gaze and hypometric saccadic eye movements in other directions. There was no blepharospasm. There were dystonic movements of the jaw with restricted jaw opening. There was mild increased tone with reinforcement in both upper limbs and a low amplitude irregular tremor with the arms outstretched. There was no rest tremor. Fine alternating movements of the fingers and finger tapping movements were slow. Reflexes were normal in the upper limbs and brisk in the lower limbs. Plantar responses were downgoing. There were no cerebellar signs and sensation was normal. On walking, there was reduced arm swing with some mild dystonic posturing, more at the wrist than at the fingers. There was mild retropulsion on pull testing. Cerebral magnetic resonance image (MRI) scan was unremarkable. Olfactory testing using brief UPSIT test showed that olfaction was markedly impaired (below 10th percentile) but an MIBG heart scan was within normal limits. He had a good response to levodopa/benserazide 200/500 tds, with improvement in both bradykinesia and rigidity. His sister presented at the age of 18 with a mouth tremor and a tendency to extend the neck. She had a past history of anxiety and depression since the age of 17 years. She also developed signs of bilateral parkinsonism with additional features of a cervical dystonia and mild long tract signs. On examination she had a mild and intermittent retrocollis and torticollis to the right. There was a facial tremor and loss of saccadic movements on upward gaze. Tone was normal. There was no rest tremor. Fractionated finger movements were slow and reduced in amplitude. Reflexes were normal in the upper limbs and brisk in the lower limbs. Plantar responses were downgoing. There were no cerebellar signs and sensation was normal. Gait was slow and there was a reduction in stride length. There was no dystonic posturing on the limbs, and postural reflexes were normal. The mother, aged 58, had no signs of Parkinsonism. The father was estranged and not available for examination. The mother's sister was available for examination, and was found to be neurologically normal. The clinical figures of the patients are compared to those of previously reported cases with KRS in Table 1. This study was approved by Northern Sydney & Central Coast Health Human Research Ethics Committee.

Identification of Mutations in ATP13A2

Mutations were identified by direct sequencing of *ATP13A2*(NM_0022089.1) and heterozygous state was confirmed by polymerase chain reaction (PCR) of exons containing mutations followed by restriction fragment-length polymorphism (RFLP). Nucleotide numbering reflects cDNA numbering with +1 corresponding to the A of the ATG translation initiation codon in the reference sequence NM_0022089.1, according to journal guidelines (www.hgvs.org/mutnomen). Initiation codon is codon 1. See Supporting Information for details.

Cloning the Full-Length ATP13A2 cDNA

Full-length *ATP13A2* cDNA was cloned with a green fluorescence protein (GFP) or V5 into a mammalian expression vector and *ATP13A2* cDNA with c.3253delC was generated by site-directed mutagenesis. See Supporting Information for details.

Cell Culture

Culture conditions for COS-7 cells, human fibroblasts, and human olfactory neurospheres (hONs) are described in Supporting Information and elsewhere [Murrell et al., 2005]. hONs were subcultured to a maximum of 10 passages for the current experiments.

Subcellular Localization of ATP13A2

COS7 cells were grown on coverslips and were transfected with *pcDNA3-ATP13A2-GFP* wild-type or *pcDNA3-ATP13A2-GFP* c.3176T>G using Lipofectamine 2000 (Invitrogen, Carlsbad, CA). One day after transfection, the cells were washed with Hank's balanced salt solution and stained with 100 nM Lysotracker Red DND-99 (Invitrogen) for 5–15 min and observed under a confocal microscope (LAS AS SP5 confocal microscope; Leica, Germany). For double immunocytochemistry, the cells were transfected with *pcDNA3-V5-tagged ATP13A2(V5-ATP13A2)* with or without mutation and allowed to grow for 2 days. In order to visualize the lysosomes clearly, the cells were treated with bafilomycin A1(BafA1) treatment, 0.5 μM BafA1 for 16 hr 1 day after transfection. The cells were stained (as described in Supporting Information) and the fluorescence was visualized using confocal microscopy.

Determination of Degradation Pathway of Mutant ATP13A2

Tagged wild-type or mutant *ATP13A2* was transfected into COS7 cells. One day after transfection, cells were treated with a proteasomal inhibitor (10 μM MG132 for 8 hr or 1 μM epoxomicin for 16 hr) or a lysosomal inhibitor (20 mM NH_4Cl for 16 hr) and subjected to Western blotting as described in the

Table 1. Clinical Features of Patients with Kufor-Rakeb Syndrome

Origin of family	Chinese	Japanese	Chilean	Jordanian	Brazilian	Italian	Afghan	Pakistan
Zygocity	Comp. hetero.	Homo.	Comp. Hetero.	Homo.	Homo.	Homo.	Homo.	Homo.
Mutation (gene)	c.3176T>G/c.3253delC	c.546C>A	c.3057delC/c.1306+5G→A	c.1632_1653dup22	c.1510G>C	c.2629G>A	c.2742_2743delTT	c.1103−1104insGA
(protein)	p.L1059/p.L1085WfsX1088	p.F182L	p.1019GfsX1021/p.G399_L435del	p.552LfsX788	p.G504R	p.G877R	p.F851CfsX856X	p.T367RfsX29
References	This paper	Kanai et al., 2009 Ning et al., 2008	Behrens et al., 2010 Kertelge et al., 2010 Ramirez et al., 2006	Kertelge et al., 2010 Williams et al., 2005	Di Fonzo et al., 2007	Santoro et al., 2010	Crosiers et al., 2010	Schneider et al., 2010
Age of onset (years)	17	22	12–18	12–15	12	10	10	16
Disease course	Rapidly deteriorating	Slowly progressive	Slowly progressive	Rapidly deteriorating	Delayed deterioration then rapidly progressive	Slowly progressive	Rapidly deteriorating	Slowly progressive
Disease duration	1–5	21	26–27	11–24	10	31	N/A	24
Initial symptoms	Social anxiety	Gait disturbance	Bradykinesia Mental retardation Rigidity	Bradykinesia Mental retardation Rigidity	Bradykinesia	Gait disturbance	Slow hand writing	Bradykinesia Mental retardation
Increased tone	+	+	+	+	+	+	+	+
Babinski sign	+	+	+	+	−	+	+	+
Bradykinesia	+	+	+/− (3/1)	+	+	+	+	+
Tremor	+	+	+	−	−	−	+	−
Rigidity	+	+	+	+	+	+	+	+
FFF minimyoclonus	+	+	+/− (3/1)	+	−	+	+	+
Slow saccade eye movement	+	+	+/− (2/1)	+	+	+	+	+
Supranuclear gaze palsy	+	+	+/− (3/1)	+	+	+	+	+
Dystonia	+	N/A	N/A	N/A	N/A	+	+	+
Pyramidal signs	+	+	+	+	+	+	+	+
Cognitive impairment/ Dementia	+	+	+	+	−	+	+	+
MMSE score	N/A	15/30	9–19/30	2–14/30	N/A	N/A	N/A	N/A
Hallucination	−	+	+/− (3/1)	+	+	−	+	−
Olfactory abnormality	+	N/A	+	+	N/A	N/A	N/A	N/A
MIBG heart scan	Normal	Normal	N/A	N/A	N/A	N/A	N/A	N/A
Other features	Lip/chin tremor Psychotic episodes	Anosmia Dysarthria Dysphagia	−	−	Lip/chin tremor Jerky facial movements Psychotic episodes	Dysarthria Dysphagia Hypomimia	Hypomimia Psychotic episodes	Anarthric, ankle clonus, chin, or tongue tremor
Response to levodopa treatment	Yes	Yes	Inconsistent response	Yes	Yes	Yes	Yes	Yes
Neuroimaging	MRI Normal	MRI Diffuse brain/spinal atrophy	MRI Mild diffuse atrophy	MRI Generalized brain atrophy	CT Diffuse brain atrophy	MRI Diffuse brain atrophy	MRI Normal	MRI Generalized brain atrophy

Comp. Hetero.; compound heterozygous; Homo.; homozygous; FFF minimyoclonus; facial-faucial-finger minimyoclonus; MIBG; metaiodobenzylguanidine; N/A; not available.
The number in the parenthesis indicates number of people affected. Nucleotide numbering reflects cDNA numbering with +1 corresponding to the A of the ATG translation initiation codon in the reference sequence NM_0022089.1, according to journal guidelines (www.hgvs.org/mutnomen). Initiation codon is codon 1.

Supporting Information. The density was measured using Image J software (version 1.38x).

Evaluation of ER Stress in hONs Using Quantitative Real-Time RT-PCR (qRT-PCR)

To determine the presence of ER stress, we measured the expression of unfolded protein response (UPR)-related genes by qRT-PCR in the hONs as described in the Supporting Information.

The genes examined here included heat-shock 70-kDa protein 5 (BiP), DNA-damage-inducible transcript 3 (CHOP), homocysteine-inducible, ER stress-inducible, ubiquitin-like domain member 1 (HERPUD1), X-box binding protein 1 (XBP1), and its spliced variant (sXBP1). Primer sequences used are listed in Supp. Table S1.

Assessment of Nonsense-Mediated mRNA Decay on ATP13A2 c.32553delC mRNA

COS7 cells transiently expressing *V5-ATP13A2* or fibroblasts derived from the proband were treated with DMSO or cycloheximide (Sigma, St. Louis, MO; 200 μg/ml, 2 hr for COS7 or 100 μg/mL, 16 hr for fibroblasts) and collected for cDNA synthesis and subsequent qRT-PCR as described in the Supporting Information. To avoid detecting endogenously expressed *ATP13A2* in COS7 cell, a pair of primers specific to V5-tagged *ATP13A2* was used. Primer sequences used are listed in Supp. Table S1.

Expression of endogenous ATP13A2 mRNA was measured by qRT-PCR. Composition of *ATP13A2* mRNA was analyzed using sequencing or RFLP on the RT-PCR product generated from the patient-derived cells as described in the Supporting Information.

Statistical Analysis

All experimental data were expressed as mean ± SD. Two-tailed *t*-test or one-way ANOVA followed by post hoc Tukey-Kramer multiple comparisons test was used to test statistical significance and a p-value of less than 0.05 was considered to be significant.

Results

Sequence Analysis of ATP13A2

Sequencing of genomic DNA from both siblings (Fig. 1A) revealed two novel compound heterozygous mutations at c.3176T>G and c.3253delC (Fig. 1B). The asymptomatic mother (Ia) was heterozygous for the c.3176T>G mutation and her sister (Ib) lacked any mutations in *ATP13A2* (Fig. 1C). The c.3176T>G and c.3253delC mutations were not present in over 150 Asian control subjects (data not shown).

The heterozygous thymine to guanine missense mutation in exon 27 at c.3176 (Fig. 1D) results in a change of a leucine to a charged arginine residue in the hydrophobic TM8 at p.1059 position in ATP13A2 (p.L1059R). The second mutation, a microdeletion of a cytosine at c.3253, was present on the other allele of *ATP13A2* and located in exon 28. This second mutation causes premature termination at position p.1088 in the middle of TM9 in ATP13A2 after addition of three erraneous amino acids from the site of the mutation (p.L1085WfsX1088).

Sequence alignments across several different species including primate, rodent, amphibian and insect (Fig. 1E) showed that the leucine at p.1059 was highly conserved among all the species with an exception for isoleucine in the fruit fly. Similarly, the leucine at p.1085 was well-conserved among mammalian species.

Wild-type ATP13A2 Localizes to the Lysosome and Mutant ATP13A2 is Retained in the Endoplasmic Reticulum

To identify the subcellular localization of mutant, we cloned wild-type and mutant *ATP13A2* with a GFP tag at the 3′ end or a V5 tag downstream of the initiation codon. For *ATP13A2* c.3253delC, only the V5 tag was used because this mutation causes a premature termination. When wild-type *ATP13A2-GFP* was expressed in COS7 cells, a green fluorescent signal was observed as numerous ring forms in the cytosol. Lysotracker, a lysosomal marker, was frequently surrounded by this signal (Supp. Fig. S1). This ring-like pattern and colocalization with Lysotracker was absent when ATP13A2-GFP c.3176T>G was expressed.

To further examine subcellular localization of mutant ATP13A2, we transiently transfected *V5-ATP13A2* into COS7 cells and performed double-labeled immunohistochemistry. To facilitate visualization of lysosomes, we used Bafilomycin A1 (BafA1), a lysosomal proton pump inhibitor, which led to the accumulation of LAMP2-positive vesicles in the cell (Fig. 2). Under BafA1 treatment, wild-type ATP13A2 was observed in LAMP2-positive vesicles with a different distribution pattern to that of LAMP2 on the same vesicle (Fig. 2C and Supp. Fig. S2). In contrast, mutant ATP13A2 was observed in a reticulum-like structure in the cytosol (Fig. 2D for ATP13A2 c.3176T>G and Fig. 2G for ATP13A2 c.3253delC) and was not localized to LAMP2-positive vesicles. The distribution pattern of mutant ATP13A2 suggested their localization in the ER and thus, we costained for V5-ATP13A2 and calreticulin, an ER marker (Fig. 3). Treatment of BafA1 did not change the localization of wild-type and mutant ATP13A2, and there was only minimal overlap observed between ATP13A2 and the ER marker in cells expressing wild-type ATP13A2 (Fig. 3C). In contrast, cells expressing mutant ATP13A2 displayed extensive colocalization with calreticulin, indicating that both mutant ATP13A2 proteins were located in the ER (Fig. 3F for ATP13A2 c.3176T>G and Figure 3I for ATP13A2 c.3253delC). A similar result was obtained when the V5-ATP13A2 detected under BafA1 treatment (Supp. Fig. S3) or when the ATP13A2-GFP was expressed instead of V5-ATP13A2 (Supp. Fig. S4).

Mutant ATP13A2 is Degraded by the Proteasomal Pathway, Not the Lysosomal Pathway, and Causes ER Stress

Mutant lysosomal proteins have previously been reported to mislocalize to the ER and undergo proteasomal degradation [Oresic et al., 2009; Ramirez et al., 2006]. This prompted us to examine whether mutant ATP13A2 in our patients was also degraded in this way. We treated COS7 cells transfected with *ATP13A2* with the proteasomal inhibitors (MG132 and epoxomicin) and the lysosomal degradation inhibitor, NH_4Cl (Fig. 4A). Consistent with mutant ATP13A2 being degraded, the amount of mutant ATP13A2 protein detected on Western blotting was less than that of wild-type ATP13A2 in untreated cells. Treatment with MG132 increased the amount of protein (fold changes over the vehicle control; 1.0 ± 0.29 for wild type, 3.6 ± 1.23 for c.3176T>G, 4.4 ± 1.44 for c.3253delC) and epoxomicin, a selective and irreversible inhibitor of proteasome, also increased the levels of the mutant proteins (1.2 ± 0.11 for wild type, 12.3 ± 2.25 for c.3176T>G, and 8.5 ± 5.67 for c.3253delC). Similar results were obtained when ATP13A2-GFP was used (data not shown). In contrast, impairment of lysosomal degradation by NH_4Cl, as indicated by the accumulation of LC3-II (Supp. Fig. S5), did not change the amount of ATP13A2 expressed (0.9 ± 0.22 for wild type, 1.5 ± 0.71 for c.3176T>G, and 1.0 ± 0.04 for c.3253delC),

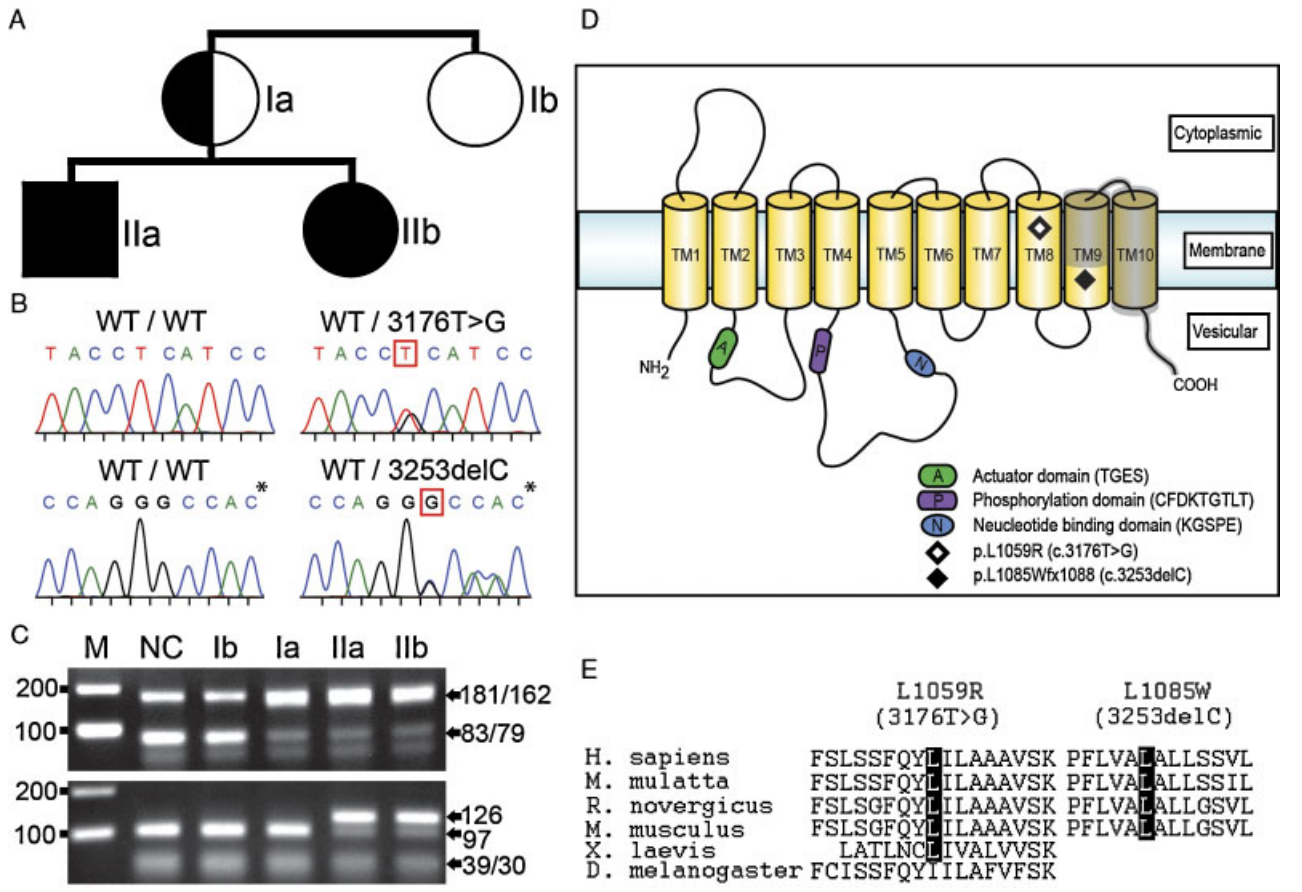

Figure 1. Identification of compound heterozygous mutations in *ATP13A2*. **A:** Family pedigree. Square symbols indicate males and circle symbols indicate females. Filled symbols indicate affected patients with compound heterozygous mutations, a half-filled symbol indicates single heterozygous mutation carriers and an open symbol indicates unaffected wild-type family members. **B:** Electropherograms of the *ATP13A2* genomic DNA from a healthy control and a patient with KRS. The c.3176T > G missense mutation in exon 27 and the c.3253delC deletion mutation in exon 28. *Reverse primer was used to detect the c.3253delC deletion mutation. **C:** RFLP analysis for *ATP13A2* in the family members. 83 and 79-bp bands are for wild-type or a 162-bp band for the c.3176T > C mutation in the top panel, while 97 and 30 bp bands are for wild type and a 126-bp band for the 3253delC mutation in the bottom panel. M, DNA marker; NC, normal control, see A for Ia, Ib, IIa, and IIb. **D:** Alignment of the ATP13A2 protein residues targeted by mutations identified in patients. GenBank access number; *Macaca mulatta* (rhesus monkey, XP_001087655), *Rattus norvegicus* (rat, XP_342963), *Mus musculus* (mouse, XP_996695), *Xenopus laevis* (*Xenopus*, AAH77611) and *Drosophila melanogaster* (fruitfly, NP_995587). **E:** Schematic modeling of ATP13A2. The location of mutations are marked by a open diamond for c.3176T > G missense mutation resulting in change of a leucine to an arginine (p.L1059R) and a filled diamond for c.3253delC deletion mutation changing a leucine to a trytophan on the site of mutation and a frameshift causing a premature termination of the protein after addition of two more erroneous amino acids (p.L1085WfsX1088). The predicted part affected by the premature termination is indicated in gray-colored shadow. [Color figures can be viewed in the online issue, which is available at www.wiley.com/humanmutation.com.]

indicating that ATP13A2 was not degraded by the lysosomal pathway. The addition of NH_4Cl to MG132-treated cells expressing mutant ATP13A2 did not further increase the amount of the protein (data not shown).

To determine whether ER retention and degradation of mutant ATP13A2 induced ER stress, we performed qRT-PCR for the UPR-related genes whose expression is known to increase during ER stress [Kaufman, 1999]. To assess the biological relevance of these changes, we used hONs, a human-derived cell model cultured from the olfactory mucosa of an affected subject. hONs have recently been reported as providing a good cell model to study the disease specific abnormalities in human brain disorders [Matigian et al., 2010; Murrell et al., 2008]. Derived from an affected patient, these cultures contain endogenous levels of mutant ATP13A2 that is responsible for causing the disease in the donor subject. Given that olfaction was impaired in our donor patient, these cell lines are particularly relevant to investigating KRS-related disease mechanisms. The expression level of all the genes examined here was significantly increased in hONs derived from the proband when compared to control (Fig. 4B); 1.3 ± 0.12-fold increase for BiP, 1.4 ± 0.17 for CHOP, 1.6 ± 0.17 for HERPUD1, 1.4 ± 0.09 for XBP1, and 1.6 ± 0.19 for sXBP1.

ATP13A2 c.3253delC mRNA was Degraded by Nonsense-Mediated mRNA Decay

Given the c.3253delC deletion mutation is predicted to cause premature termination of ATP13A2, we tested whether NMD contributed to the degradation of mutant mRNA. NMD is a protective mechanism that removes defective mRNA containing early termination mutations to protect the cell from truncated and functionally abnormal proteins [Maquat and Gong, 2009]. NMD starts from the pioneer step of translation and it can be attenuated by using inhibitors of protein synthesis such as cycloheximide. Wild-type or mutant *V5-ATP13A2* was expressed in COS7 and its cDNA level was examined by qRT-PCR using primers specific to

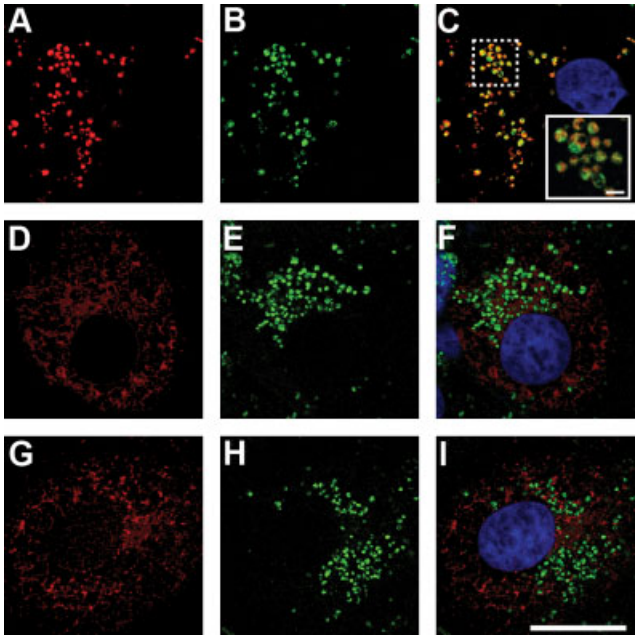

Figure 2. Localization of wild-type and mutant ATP13A2 protein under Bafilomycin A1 treatment. Wild-type or mutant V5-tagged ATP13A2 (red) was expressed in COS7 cell and subsequently costained with LAMP2 (green) after Bafilomycin A1 treatment. Bafilomycin A1 treatment induced accumulation of LAMP2-positive vesicles in the cell (**B**, **E**, and **H**). Wild-type ATP13A2 (**A**) was colocalized with LAMP2 in the same vesicle (**C**). Inset (solid white outlined box in figure **C**) shows magnified view of the area outlined in dotted white outlined box. Bar in inset: 2 μm. In contrast, both ATP13A2 c.3176T > G (middle panel, **D–F**) and c.3253delC (bottom panel, **G–I**) showed a peri-nuclear reticular staining pattern in the cytosol. Mutant ATP13A2 did not colocalize with LAMP2 (**F** for c.3176T > G and **I** for c.3253delC). Nuclei were stained with DAPI (blue). Bar: 20 μm.

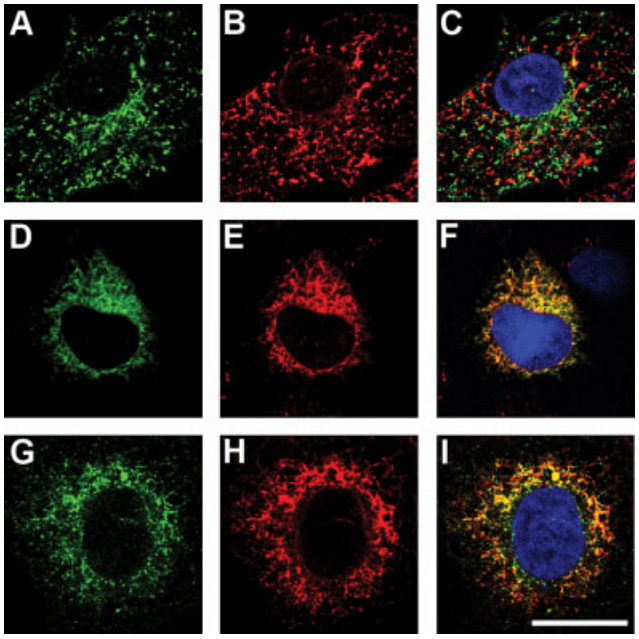

Figure 3. Localization of mutant ATP13A2 protein in the endoplasmic reticulum. COS7 cells were transiently transfected with V5-tagged *ATP13A2* and stained for V5 (green) and calreticulin (red), an endoplasmic reticulum marker using double immunocytochemistry. Wild-type ATP13A2 (**A**) showed minimal overlapping with calreticulin (**C**), while ATP13A2 c.3176T > G mutation (**D**) or c.3253delC mutation (**G**) colocalized with the endoplasmic reticulum marker (**F** for c.3176T > G and **I** for c.3253delC). Nuclei were stained with DAPI (blue). Bar: 20 μm.

the transfected gene. The expression level of *ATP13A2* c.3253delC was significantly decreased compared to the wild-type while that of *ATP13A2* c.3176T > G was not changed (Fig. 5A). After treatment with cycloheximide, the expression level of *ATP13A2* c.3253delC was recovered to that of wild-type *ATP13A2*, indicating that NMD plays a role in the degradation of *ATP13A2* c.3253delC mRNA. To determine mRNA expression of mutant *ATP13A2* in physiologically relevant conditions, we performed qRT-PCR for *ATP13A2* using hONs from the proband. We found significantly decreased expression of *ATP13A2* mRNA in the patient hONs (0.7 ± 0.08 in fold change) compared to the control (Fig. 5B). When the composition of mutant *ATP13A2* mRNA was examined by sequencing (Fig. 5C) and RFLP analysis (Fig. 5D) using a fragment amplified by RT-PCR, the majority of *ATP13A2* mRNA in the patient-derived cells was accounted for by c.3176T > G with the level of *ATP13A2* c.3253delC mRNA being partially recovered by cycloheximide treatment.

Discussion

We report a family with two siblings with typical clinical features of KRS. We found novel compound heterozygous mutations: c.3176T > G missense mutation (p.L1059R) and a c.3253delC deletion mutation (p.L1085WfsX1088), in *ATP13A2*. Using a transient transfection model and human, patient-derived cell models, we demonstrate that these mutations cause retention of ATP13A2 in the ER, ER stress, and degradation by the endoplasmic reticulum-associated protein degradation (ERAD)-proteasomal pathway. We also show the mutation causing premature termination results in NMD. These findings indicate that the novel mutations identified in our patients with KRS are pathogenic by causing loss of function of the ATP13A2 and implicate that several different mechanisms are involved in the etiology of KRS. Our proband and his sister both had early onset, levodopa-responsive parkinsonism with additional atypical parkinsonian features such as pyramidal signs, supranuclear gaze palsy, dystonia, and behavioural disturbances, manifestations typical of the clinical features of KRS. Similar to other reports, additional testing in our proband showed that olfaction was impaired [Kertelge et al., 2010], but the MIBG heart scan was within normal limits [Kanai et al., 2009]. Cerebral MRI showed no evidence of iron accumulation [Schneider et al., 2010].

Both novel mutations identified in the affected family members disrupted well-conserved mammalian residues within *ATP13A2* (Fig. 1), which likely result in misfolding and subsequent mislocalization of the ATP13A2 protein (see below).

Our studies showed that wild-type ATP13A2 is located in lysosomes, as overexpressed wild-type ATP13A2 colocalized with lysosomal markers, Lysotracker and LAMP2 (Fig. 2 and Supp. Fig. S1). By treating cells with BafA1 for a period of time known to inhibit the fusion of autophagosomes with both late endosomes and lysosomes [Klionsky et al., 2008; Yamamoto et al., 1998], we found that LAMP2-positive lysosomes accumulated and V5-tagged wild-type ATP13A2 colocalized with the lysosomes albeit with a different distribution pattern to that of LAMP2. Previously, ATP13A2 has been reported to be in the lysosomal membrane as shown by colocalization of a tagged ATP13A2 with lysosomal markers [Ramirez et al., 2006] and untagged ATP13A2 protein in the lysosomal membrane fraction [Schroder

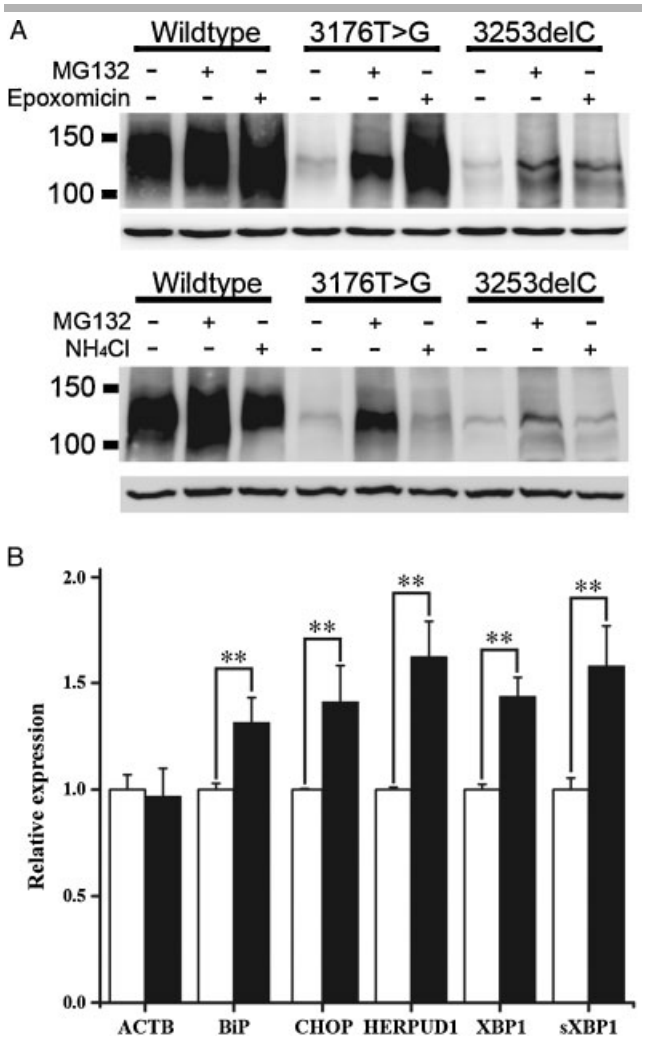

Figure 4. Mutant ATP13A2 is degraded by proteosomal pathway and causes consistent ER stress in the patient-derived cell. **A:** COS7 cells expressing V5-tagged ATP13A2 were treated with either DMSO or a proteasomal inhibitor (MG132; 10 μM for 8 hr or epoxomicin; 1 μM for 24 hr) or a lysosomal inhibitor (NH_4Cl; 20 mM for 24 hr) and their protein was extracted and stained for V5 in a Western blot. The amount of protein was markedly increased for both mutant ATP13A2 species after exposure to MG132 (fold changes compared to vehicle control, 3.6 ± 1.23 for c.3176T > G and 4.4 ± 1.44 for c.3253delC) or epoxomicin (12.3 ± 2.25 for c.3176T > G and 8.47 ± 5.67 for c.3253delC), whereas there was no change for the wild-type counterpart (1.0 ± 0.29 for MG132 and 1.2 ± 0.11 for epoxomicin). In comparison, NH_4Cl did not protect the degradation of mutant proteins (0.9 ± 0.22 for wild type, 1.5 ± 0.71 for c.3176T > G, and 1.0 ± 0.04 for c.3253delC). Fold changes were calculated from three independent Western blot images and a representative image is shown. **B:** To examine for evidence of ER stress, the expression level of unfolded protein response-related genes was examined using hONs. The expression level of all the genes examined was significantly increased in hONs derived from the proband (filled bar) compared to control (open bar); 1.3 ± 0.12 fold increase for BiP, 1.4 ± 0.17 for CHOP, 1.6 ± 0.17 for HERPUD1, 1.4 ± 0.09 for XBP1, and 1.6 ± 0.19 for sXBP1. $^{**}P < 0.01$ for all in two-tailed Student *t*-test. For abbreviations, see Materials and Methods.

et al., 2007]. Our findings confirm that wild-type ATP13A2 is located in the lysosome.

The novel mutations identified in our patients dramatically changed the localization of mutant ATP13A2. ATP13A2 c.3176T > G was observed throughout cytoplasm without a defined pattern while wild-type ATP13A2 formed ring structures in the lysosomal membrane (Supp. Fig. S1). Mutant ATP13A2 did not localize to lysosomes and instead formed a peri-nuclear reticulum with colocalization to the ER (Figs. 2–3 and Supp. Figs. S3–S4).

Proteins with a complex tertiary structure need to fold properly to achieve normal localization and function in the target organelle, whereas misfolded proteins may be retained in the ER and subjected to premature degradation [Rao and Bredesen, 2004]. Both novel mutations identified in the affected family members would be expected to cause misfolding as they disrupt well conserved regions of the mammalian *ATP13A2*. We found that these mutant ATP13A2 were localized to the ER suggesting misfolding of ATP13A2 due to missense or truncation mutations.

Misfolded proteins in the ER are rapidly degraded by the proteasome-dependent ERAD machinery [Kincaid and Cooper, 2007]. Consistent with this, the steady-state level of mutant ATP13A2 protein expression in this study was much less than that of wild-type, and level of the mutant protein was significantly increased by proteasomal inhibition (Fig. 4A). Conversely, lysosomal inhibition did not protect them from degradation at a dose adequate for effective inhibition of lysosomal function, that is, accumulation of LC3-II (Supp. Fig. S5) (see Fu et al. [2009]). These data strongly suggest that ATP13A2 is degraded by the proteasomal pathway, not by the lysosomal pathway and that mutant ATP13A2 is rapidly removed by the proteasomal pathway.

Misfolded proteins in the ER cause ER stress, which in turn activates the UPR, a mechanism that can upregulate ERAD to remove the ER stress. To examine the activation of UPR following ER stress possibly caused by mutant ATP13A2, we used hONs established from nose biopsies of the proband and compared the expression level of UPR-related genes by qRT-PCR to control cells (Fig. 4B). All genes examined, BiP (an ER chaperone and regulator of the UPR), CHOP (a transcription factor that mediates ER stress), HERPUD1 (a ubiquitin-like membrane protein induced by ER stress), XBP1 (a potent UPR transcription factor), and sXBP1 (a splice variant of XBP1 formed on UPR activation), showed significant increases in gene expression, indicating persistent ER stress was caused by endogenous mutant ATP13A2 in our patient-derived cell model.

Early termination at p.1088 in *ATP13A2* c.3253delC suggested degradation of *ATP13A2* mRNA might contribute to its reduced protein expression. To test involvement of NMD in degradation of *ATP13A2* mRNA, we performed qRT-PCR specific for *ATP13A2* in both the transient transfection system and in the hONs-cell model (Fig. 5). The expression level of *ATP13A2* c.3253delC mRNA was significantly reduced compared to wild-type or *ATP13A2* c.3176T > G mRNA and treatment of cycloheximide fully recovered the *ATP13A2* c.3253delC mRNA level. We confirmed that the majority of *ATP13A2* mRNA in the patient hONs and fibroblasts was with c.3176T > G and cycloheximide partially recovered the level of *ATP13A2* c.3253delC mRNA. These findings indicate that NMD is involved in degradation of *ATP13A2* c.3253delC mRNA and thus plays a role in the pathogenesis of KRS.

The present study demonstrates several different mechanisms by which mutations in ATP13A2 may contribute to the development of KRS. However, it is possible that other mechanisms may also contribute to the onset and progression of the disease. First, pathogenic mutations in ATP13A2 failing to reach the lysosome may result in impaired lysosomal function. This effect may lead to the cellular accumulation of unnecessary or toxic proteins such as α-synuclein, a protein known to accumulate and contribute to the aetiology of PD. Recently, the lysosomal pathways have been shown to be involved in the degradation of α-synuclein [Vogiatzi et al., 2008] and overexpression of ATP13A2

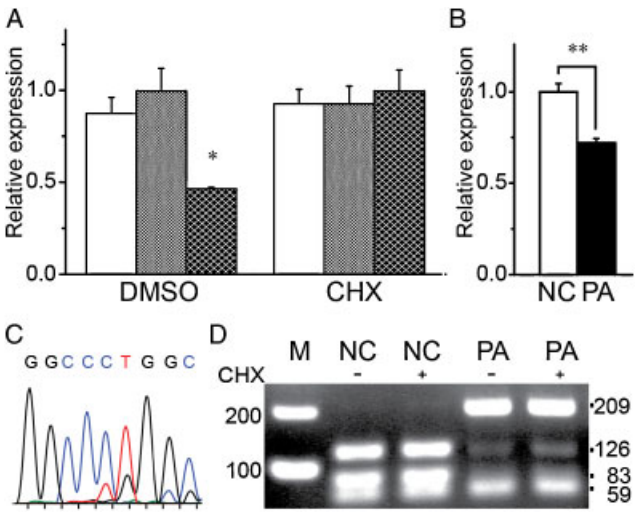

Figure 5. Nonsense-mediated mRNA decay of *ATP13A2* c.3253delC mRNA. COS7 cells were transiently transfected with V5-tagged *ATP13A2* and subjected to quantitative real-time RT-PCR (qRT-PCR) to measure the level of V5-tagged *ATP13A2* mRNA. **A:** The mRNA level of V5-tagged *ATP13A2* c.3253delC (darker shaded bar) was significantly decreased compared to wild-type *ATP13A2* (open bar), whereas no change was detected in the level of *ATP13A2* c.3176T > G cDNA (lighter shaded bar). Treatment of cycloheximide restored the expression of *ATP13A2* with the deletion mutation to the level of wild-type *ATP13A2*. $^{*}P < 0.05$ in one-way ANOVA followed by Tukey-Kramer multiple comparison test. **B:** The expression level of *ATP13A2* mRNA was examined in human olfactory neurospheres (hONs) by qRT-PCR; the level of *ATP13A2* was significantly lower in the hONs of the patient (dark filled bar) when compared to control (white bar). $^{**}P < 0.01$ in two-tailed Student *t*-test. NC, control; PA, patient. **C:** The electropherogram for mutant *ATP13A2* in the patient hONs. A fragment in *ATP13A2* was amplified in RT-PCR and subjected to sequencing. The peak height on the eletropherogram for *ATP13A2* c.3253delC was smaller than that of *ATP13A2* c.3176T > G. **D:** RFLP analysis of wild-type *ATP13A2* cDNA at the position of c.3176 results in 126/83-bp bands, whereas there is a loss of restriction site if mutant c.3176T > G is present, resulting in a single 209-bp band. For *ATP13A2* from the patient-derived fibroblasts, the 126/83 bp indicate *ATP13A2* c.3253delC mRNA. RFLP analysis showed majority of *ATP13A2* mRNA in the patient cells was accounted for by *ATP13A2* c.3176T > G mRNA and treatment of cycloheximide (100 μg/ml for 16 hr) partially recovered level of the mRNA, whereas the same treatment did not change the amount of wild-type mRNA. M, DNA marker; NC, control; PA, patient. [Color figures can be viewed in the online issue, which is available at www.wiley.com/humanmutation.com.]

in rat primary midbrain dopaminergic neurons suppressed α-synuclein toxicity [Gitler et al., 2009]. Second, the observation that the mutant ATP13A2 is degraded by the proteasomal pathway raises the possibility that mutant species might overload the proteasomal pathways and disturb its normal function to degrade other proteins, particularly if the lysosomal pathways are not working efficiently. The importance of the proteasomal pathway in the pathogenesis of parkinsonism has already been implicated in other cases of familial PD associated with Parkin and UCHL1 [Kitada et al., 1998; Leroy et al., 1998]. Other mechanisms that have been reported to play a role in the aetiology of KRS include impaired ion transportation or ionic imbalance that results in increased oxidative stress in the cell [Gitler et al., 2009; Schmidt et al., 2009].

Elucidating the molecular disturbances that occur in patients with genetic forms of parkinsonism is critical to developing alternative therapeutic measures. Here, we report a family affected by KRS, an atypical early-onset form of parkinsonism associated with novel mutations identified in *ATP13A2*. We demonstrate that the mutations are pathogenic using mammalian and patient-derived cell models. Further study will be needed to understand the function of ATP13A2 in physiological and pathological conditions, and this would be beneficial to understand other types of parkinsonism including Parkinson disease.

Acknowledgments

We thank Dr. Neil Manwaring and Ingrid Goebel for technical assistance and Wendy Welsh for clinical assistance.

References

Behrens MI, Brüggemann N, Chana P, Venegas P, Kägi M, Parrao T, Orellana P, Garrido C, Rojas CV, Hauke J, Hahnen E, González R, Seleme N, Fernández V, Schmidt A, Binkofski F, Kömpf D, Kubisch C, Hagenah J, Klein C, Ramirez A. 2010. Clinical spectrum of Kufor-Rakeb syndrome in the Chilean kindred with ATP13A2 mutations. Mov Disord 25:1929–1937.

Bonifati V, Rizzu P, van Baren MJ, Schaap O, Breedveld GJ, Krieger E, Dekker MCJ, Squitieri F, Ibanez P, Joosse M, van Dongen JW, Vanacore N, van Swieten JC, Brice A, Meco G, van Duijn CM, Oostra BA, Heutink P. 2003. Mutations in the DJ-1 gene associated with autosomal recessive early-onset Parkinsonism. Science 299:256–259.

Crosiers D, Ceulemans B, Meeus B, Nuytemans K, Pals P, Van Broeckhoven C, Cras P, Theuns J. 2011. Juvenile dystonia-parkinsonism and dementia caused by a novel ATP13A2 frameshift mutation. Parkinsonism Relat Dis 17:135–138.

Di Fonzo AM, Chien HFM, Socal MM, Giraudo SB, Tassorelli CM, Iliceto GM, Fabbrini GM, Marconi RM, Fincati EM, Abbruzzese GM, Marini P, Squitieri F, Horstink MW, Montagna P, Libera AD, Stocchi F, Goldwurm S, Ferreira JJ, Meco G, Martignoni E, Lopiano L, Jardim LB, Oostra BA, Barbosa ER, Italian Parkinson Genetics Network, Bonifati V. 2007. ATP13A2 missense mutations in juvenile parkinsonism and young onset Parkinson disease. Neurology 68: 1557–1562.

Fu L, Kim Y-A, Wang X, Wu X, Yue P, Lonial S, Khuri FR, Sun S-Y. 2009. Perifosine inhibits mammalian target of rapamycin signaling through facilitating degradation of major components in the mTOR axis and induces autophagy. Cancer Res 69:8967–8976.

Gitler AD, Chesi A, Geddie ML, Strathearn KE, Hamamichi S, Hill KJ, Caldwell KA, Caldwell GA, Cooper AA, Rochet J-C, Lindquist S. 2009. Alpha-Synuclein is part of a diverse and highly conserved interaction network that includes PARK9 and manganese toxicity. Nat Genet 41:308–315.

Hatano T, Kubo S-i, Sato S, Hattori N. 2009. Pathogenesis of familial Parkinson's disease: new insights based on monogenic forms of Parkinson's disease. J Neurochem 111:1075–1093.

Kanai K, Asahina M, Arai K, Tomiyama H, Kuwabara Y, Uchiyama T, Sekiguchi Y, Funayama M, Kuwabara S, Hattori N, Hattori T. 2009. Preserved cardiac ^{123}I-MIBG uptake and lack of severe autonomic dysfunction in a PARK9 patient. Mov Disord 24:1403–1404.

Kaufman RJ. 1999. Stress signaling from the lumen of the endoplasmic reticulum: coordination of gene transcriptional and translational controls. Gene Dev 13: 1211–1233.

Kertelge L, Brüggemann N, Schmidt A, Tadic V, Wisse C, Dankert S, Drude L, van der Vegt J, Siebner H, Pawlack H, Pramstaller PP, Behrens MI, Ramirez A, Reichel D, Buhmann C, Hagenah J, Klein C, Lohmann K, Kasten M. 2010. Impaired sense of smell and color discrimination in monogenic and idiopathic Parkinson's disease. Mov Disord 25:2665–2669.

Kincaid MM, Cooper AA. 2007. ERADicate ER stress or die trying. Antioxid Redox Signal 9:2373–2387.

Kitada T, Asakawa S, Hattori N, Matsumine H, Yamamura Y, Minoshima S, Yokochi M, Mizuno Y, Shimizu N. 1998. Mutations in the parkin gene cause autosomal recessive juvenile parkinsonism. Nature 392:605–608.

Klionsky DJ, Elazar Z, Seglen PO, Rubinsztein DC. 2008. Does bafilomycin A1 block the fusion of autophagosomes with lysosomes? Autophagy 4:849–850.

Leroy E, Boyer R, Auburger G, Leube B, Ulm G, Mezey E, Harta G, Brownstein MJ, Jonnalagada S, Chernova T, Dehejia A, Lavedan C, Gasser T, Steinbach PJ, Wilkinson KD, Polymeropoulos MH. 1998. The ubiquitin pathway in Parkinson's disease. Nature 395:451–452.

Maquat LE, Gong C. 2009. Gene expression networks: competing mRNA decay pathways in mammalian cells. Biochem Soc Trans 37:1287–1292.

Matigian N, Abrahamsen G, Sutharsan R, Cook AL, Vitale AM, Nouwens A, Bellette B, An J, Anderson M, Beckhouse AG, Bennebroek M, Cecil R, Chalk AM, Cochrane J, Fan Y, Féron F, McCurdy R, McGrath JJ, Murrell W, Perry C, Raju J, Ravishankar S, Silburn PA, Sutherland GT, Mahler S,

Mellick GD, Wood SA, Sue CM, Wells CA, Mackay-Sim A. 2010. Disease-specific, neurosphere-derived cells as models for brain disorders. Dis Model Mech 3:785–798.

Murrell W, Feron F, Wetzig A, Cameron N, Splatt K, Bellette B, Bianco J, Perry C, Lee G, Mackay-Sim A. 2005. Multipotent stem cells from adult olfactory mucosa. Dev Dyn 233:496–515.

Murrell W, Wetzig A, Donnellan M, Feron F, Burne T, Meedeniya A, Kesby J, Bianco J, Perry C, Silburn P, Mackay-Sim A. 2008. Olfactory mucosa is a potential source for autologous stem cell therapy for Parkinson's disease. Stem Cells 26: 2183–2192.

Ning YP, Kanai K, Tomiyama H, Li Y, Funayama M, Yoshino H, Sato S, Asahina M, Kuwabara S, Takeda A, Hattori T, Mizuno Y, Hattori N. 2008. PARK9-linked parkinsonism in eastern asia: Mutation detection in *ATP13A2* and clinical phenotype. Neurology 70:1491–1493.

Oresic K, Mueller B, Tortorella D. 2009. Cln6 mutants associated with neuronal ceroid lipofuscinosis are degraded in a proteasome-dependent manner. Biosci Rep 29:173–181.

Polymeropoulos MH, Lavedan C, Leroy E, Ide SE, Dehejia A, Dutra A, Pike B, Root H, Rubenstein J, Boyer R, Stenroos ES, Chandrasekharappa S, Athanassiadou A, Papapetropoulos T, Johnson WG, Lazzarini AM, Duvoisin RC, Di Iorio G, Golbe LI, Nussbaum RL. 1997. Mutation in the alpha-synuclein gene identified in families with Parkinson's disease. Science 276:2045–2047.

Ramirez A, Heimbach A, Grundemann J, Stiller B, Hampshire D, Cid LP, Goebel I, Mubaidin AF, Wriekat A-L, Roeper J, Al-Din A, Hillmer AM, Karsak M, Liss B, Woods CG, Behrens MI, Kubisch C. 2006. Hereditary parkinsonism with dementia is caused by mutations in *ATP13A2*, encoding a lysosomal type 5 P-type ATPase. Nat Genet 38:1184–1191.

Rao RV, Bredesen DE. 2004. Misfolded proteins, endoplasmic reticulum stress and neurodegeneration. Curr Opin Cell Biol 16:653–662.

Santoro L, Breedveld G, Manganelli F, Iodice R, Pisciotta C, Nolano M, Punzo F, Quarantelli M, Pappatà S, Di Fonzo A, Oostra BA, Bonifati V. 2011. Novel *ATP13A2* (*PARK9*) homozygous mutation in a family with marked phenotype variability. Neurogenetics 12:33–39.

Schmidt K, Wolfe DM, Stiller B, Pearce DA. 2009. Cd2+, Mn2+, Ni2+ and Se2+ toxicity to Saccharomyces cerevisiae lacking YPK9p the orthologue of human ATP13A2. Biochem Biophys Res Commun 383:198–202.

Schneider SA, Paisan-Ruiz C, Quinn NP, Lees AJ, Houlden H, Hardy J, Bhatia KP. 2010. *ATP13A2* mutations (PARK9) cause neurodegeneration with brain iron accumulation. Mov Disord 25:979–984.

Schroder B, Wrocklage C, Pan C, Jager R, Kosters B, Schafer H, Elsasser H-P, Mann M, Hasilik A. 2007. Integral and associated lysosomal membrane proteins. Traffic 8:1676–1686.

Schultheis PJ, Hagen TT, O'Toole KK, Tachibana A, Burke CR, McGill DL, Okunade GW, Shull GE. 2004. Characterization of the P5 subfamily of P-type transport ATPases in mice. Biochem Biophys Res Commun 323:731–738.

Valente EM, Abou-Sleiman PM, Caputo V, Muqit MMK, Harvey K, Gispert S, Ali Z, Del Turco D, Bentivoglio AR, Healy DG, Albanese A, Nussbaum R, González-Maldonado R, Deller T, Salvi S, Cortelli P, Gilks WP, Latchman DS, Harvey RJ, Dallapiccola B, Auburger G, Wood NW. 2004. Hereditary early-onset Parkinson's disease caused by mutations in *PINK1*. Science 304:1158–1160.

Vogiatzi T, Xilouri M, Vekrellis K, Stefanis L. 2008. Wild type alpha-synuclein is degraded by chaperone-mediated autophagy and macroautophagy in neuronal cells. J Biol Chem 283:23542–23556.

Williams DR, Hadeed A, al-Din ASN, Wreikat A-L, Lees AJ. 2005. Kufor Rakeb Disease: autosomal recessive, levodopa-responsive parkinsonism with pyramidal degeneration, supranuclear gaze palsy, and dementia. Mov Disord 20: 1264–1271.

Yamamoto A, Tagawa Y, Yoshimori T, Moriyama Y, Masaki R, Tashiro Y. 1998. Bafilomycin A1 prevents maturation of autophagic vacuoles by inhibiting fusion between autophagosomes and lysosomes in rat hepatoma cell line, H-4-II-E cells. Cell Struct Funct 23:33–42.

Zimprich A, Biskup S, Leitner P, Lichtner P, Farrer M, Lincoln S, Kachergus J, Hulihan M, Uitti RJ, Calne DB, Stoessl AJ, Pfeiffer RF, Patenge N, Carbajal IC, Vieregge P, Asmus F, Müller-Myhsok B, Dickson DW, Meitinger T, Strom TM, Wszolek ZK, Gasser T. 2004. Mutations in *LRRK2* cause autosomal-dominant parkinsonism with pleomorphic pathology. Neuron 44:601–607.